Inversion of de Haas–van Alphen Data on Nearly Ellipsoidal Surfaces. Application to As and Sb†

J. B. KETTERSON AND L. R. WINDMILLER
Argonne National Laboratory, Argonne, Illinois 60439
(Received 25 July 1969; revised manuscript received 10 September 1969)

A transformation theorem, relating de Haas–van Alphen areas and radii under a spherical mapping of nearly ellipsoidal Fermi surfaces, has been developed. The transformation greatly increases the convergence of the spherical harmonic expansions used to parametrize these surfaces. The theorem has been applied to invert the L-centered electron surfaces of arsenic and antimony.

INTRODUCTION

IT is well known that the de Haas–van Alphen (dHvA) effect measures extremal cross-sectional areas of the Fermi surface. The question naturally arises whether the specification of the angular dependence of the extremal areas on a given sheet of the Fermi surface (FS) is sufficient information to deduce the actual shape of the surface. Lifshitz and Pogorelov[1] have shown that this inversion is indeed possible, provided the surface in question satisfies two conditions. The surface must (a) have a center of inversion symmetry and (b) have only a single-valued radius vector measured from this center. As originally formulated, the theorem was awkward to apply in practice, and Mueller[2] has recently reformulated the theorem in such a way as to simplify greatly its application. The equivalence of the Mueller and Lifshitz-Pogorelov formulation was demonstrated by Foldy.[3] The theorem was extended to cover the inversion of dHvA effective-mass data into Fermi velocities by Ketterson, Windmiller, Hörnfeldt, and Mueller.[4]

We expand the square of the radius vector $r^2(\theta,\varphi)$ (measured from the inversion center) and the extremal area $A(\theta,\varphi)$ (of the orbit whose plane contains the inversion center) in real spherical harmonics

$$r^2(\theta,\varphi)=\sum_{l,m}[\gamma_{l,m}{}^g C_{l,m}{}^g(\theta,\varphi)+\gamma_{l,m}{}^u C_{l,m}{}^u(\theta,\varphi)], \quad (1)$$

$$A(\theta,\varphi)=\sum_{l,m}[\beta_{l,m}{}^g C_{l,m}{}^g(\theta,\varphi)+\beta_{l,m}{}^u C_{l,m}{}^u(\theta,\varphi)]. \quad (2)$$

The real spherical harmonics are defined in terms of the complex spherical harmonics $Y_{l,m}(\theta,\varphi)$ by the relations

$$C_{l,m}{}^g=(1/\sqrt{2})(Y_{l,m}+Y_{l,-m}), \quad (3a)$$

$$C_{l,m}{}^u=(1/i\sqrt{2})(Y_{l,m}-Y_{l,-m}), \quad (3b)$$

$$C_{l,0}=Y_{l,0}.$$

The letters g and u refer to functions which are symmetric and antisymmetric, respectively, under the transformation $\varphi\rightarrow-\varphi$. What Mueller showed is that the relation between the coefficients in (1) and (2) is given by

$$\beta_{l,m}=\pi P_l(0)\gamma_{l,m}. \quad (4)$$

SYMMETRY CONSIDERATIONS

The requirement of inversion symmetry allows only even l in (1) and (2) since the parity of spherical harmonics is given by $(-1)^l$. Table I lists those of the 32 crystal point groups which contain the inversion operator. In the following we define the z axis as the axis of highest symmetry from which the polar angle θ is measured, x as the orthogonal axis from which the azimuthal angle φ is measured, and y as the mutually perpendicular third axis. The allowed values of m depend on the point group symmetry of the surface. For the group S_2 there is no axis of symmetry and so the z axis may be chosen arbitrarily. All values of m (from 0 to l) are included and both symmetric (g) and antisymmetric (u) coefficient appear. For the group C_{2h} the z axis is chosen as the twofold axis, and the fact that the z axis is a twofold axis requires that m be even. Both symmetric and antisymmetric coefficients appear and the x axis may be chosen arbitrarily in the plane perpendicular to z. For the group V_h we choose the x, y, and z axes to coincide with the three twofold axes; m is even and, since the x axis lies in a mirror plane, only symmetric coefficients appear. The fourfold axis is chosen as the z axis for the groups C_{4h} and D_{4h} and $m=0, 4, 8, \ldots$, i.e., $m=0$ (mod 4). The x axis is chosen to lie within one of the two nonequivalent mirror planes for D_{4h} and thus only symmetric coefficients appear. The choice of the x axis is arbitrary for C_{4h}

TABLE I. Crystal point groups having inversion symmetry.

System	International	Schoenflies
Triclinic	$\bar{1}$	$S_i(S_2)$
Monoclinic	$2/m$	C_{2h}
Orthorhombic	mmm	$D_{2h}(V_h)$
Tetragonal	$4/m$	C_{4h}
	$4/mmm$	D_{4h}
Trigonal	$\bar{3}$	$C_{3i}(S_6)$
	$\bar{3}m$	D_{3d}
Hexagonal	$6/m$	C_{6h}
	$6/mmm$	D_{6h}
Cubic	$m3m$	O_h

† Based on work performed under the auspices of the U. S. Atomic Energy Commission.
[1] I. M. Lifshitz and A. V. Pogorelov, Dokl. Akad. Nauk SSSR **96**, 1143 (1954).
[2] F. M. Mueller, Phys. Rev. **148**, 636 (1966).
[3] L. L. Foldy, Phys. Rev. **170**, 670 (1968).
[4] J. B. Ketterson, L. R. Windmiller, S. Hörnfeldt, and F. M. Mueller, Solid State Commun. **6**, 851 (1968).

and symmetric and antisymmetric coefficients appear. For the groups S_6 and D_{3d} the threefold axis is chosen as the z axis and $m=0 \pmod 3$. The x axis lies within the mirror plane for D_{3d} and only symmetric coefficients appear. The choice of the x axis is arbitrary for S_6 and symmetric and antisymmetric coefficients appear. The z axis coincides with the sixfold axis for C_{6h} and D_{6h} and $m=0 \pmod 6$. The x axis for D_{6h} is chosen to lie within one of the two nonequivalent mirror planes intersecting the x-y plane and only symmetric coefficients appear. The x axis is arbitrary for C_{6h} and both symmetric and antisymmetric coefficients appear. The group O_h requires special consideration and has been treated elsewhere.[5]

It is well known that a small FS centered on a point in the Brillouin zone having inversion symmetry is nearly ellipsoidal. For the group S_2, the ellipsoid has an arbitrary orientation and the three principal axes are nonequivalent. The specification of this ellipsoid requires six parameters (a symmetric second-rank tensor). For the group C_{2h} the z axis lies along one of the principal axes. The two nonequivalent remaining principal axes are in general rotated by an angle φ_0 in the x-y plane relative to the x and y axis. The specification of this ellipsoid thus requires four parameters. For the group V_h the three nonequivalent principal axes coincide with the x, y, and z axes and there are thus three independent parameters. For the groups C_{4h}, D_{4h}, S_6, D_{3d}, C_{6h}, and D_{6h} the ellipsoid is an ellipsoid of revolution about the z axis and the specification requires two parameters. For the cubic case (O_h) the ellipsoid degenerates to a sphere and thus requires a one-parameter specification.

AREAS AND RADII UNDER A SPHERICAL MAPPING

An inherent weakness in the expansion scheme of Mueller[2] is that the expansions (1) and (2) do not terminate after a finite number of terms for an ellipsoid. This shortcoming can be effectively circumvented, however, by performing a mathematical transformation on the coordinate system which maps the ellipsoid into a sphere and thus for a perfect ellipsoid the expansions terminate after the first term. The higher terms in the expansion can then be used to fit departures from ellipticity. We will refer to the transformation which maps an ellipsoid into a sphere as a spherical mapping and the problem at hand is to determine how the radii and areas behave under such a mapping.

The orientation of the S_2 group ellipsoid may be specified by three independent parameters (e.g., the three Euler angles) and we can perform a series of rotations on our coordinate systems so that x, y, and z axes coincide with the principal axis of the ellipsoid (principal axis transformation). Similarly, a single rotation about the z axis by an angle φ_0 aligns the C_{2h} group ellipsoid. We will thus confine ourselves, for simplicity, to a coordinate system aligned with the principal axis of the ellipsoid. The equation of such an ellipsoid is

$$x^2/a^2+y^2/b^2+z^2/c^2=1. \tag{5}$$

If we define $\alpha \equiv b/a$ and $\gamma \equiv b/c$ then the following transformation maps the ellipsoid into a sphere of radius b:

$$x'=\alpha x, \tag{6a}$$

$$y'=y, \tag{6b}$$

$$z'=\gamma z. \tag{6c}$$

We express this transformation formally by writing $T(x,y,z)=(x',y',z')$ or in polar coordinates $T(r,\theta,\varphi)=(r',\theta',\varphi')$. Similarly, $T^{-1}(x',y',z')=(x,y,z)$ and $T^{-1}(r',\theta',\varphi')=(r,\theta,\varphi)$. A small amount of algebra yields the following relations:

$$|r'(\theta',\varphi')|=|r(\theta,\varphi)|[\sin^2\theta(\sin^2\varphi+\alpha^2\cos^2\varphi)+\gamma^2\cos^2\theta]^{1/2}, \tag{7a}$$

$$\cos\varphi'=\frac{\alpha\cos\varphi}{(\sin^2\varphi+\alpha^2\cos^2\varphi)^{1/2}}, \tag{7b}$$

$$\cos\theta'=\frac{\gamma\cos\theta}{[\sin^2\theta(\sin^2\varphi+\alpha^2\cos^2\varphi)+\gamma^2\cos^2\theta]^{1/2}}. \tag{7c}$$

Now the extremal area in the plane normal to a unit vector $\hat{\xi}(\theta_0,\varphi_0)$ is given by[1]

$$A(\theta_0,\varphi_0)=\frac{1}{2}\int\delta[\hat{\xi}(\theta_0,\varphi_0)\cdot\hat{r}(\theta,\varphi)]r^2(\theta,\varphi)\sin\theta\,d\theta\,d\varphi. \tag{8}$$

It turns out to be convenient to evaluate the area in the transformed (primed) system in terms of angles measured in the untransformed (unprimed) system, i.e.,

$$A'(\theta_0,\varphi_0)=\frac{1}{2}\int\delta[\hat{\xi}(\theta_0,\varphi_0)\cdot\hat{r}(\theta',\varphi')]r'^2(\theta',\varphi')\times\sin\theta'd\theta'd\varphi'. \tag{9}$$

The integrand is a function of $(\theta_0,\varphi_0,r',\theta',\varphi')$ and we now evaluate it in terms of $(\theta_0',\varphi_0',r,\theta,\varphi)$. After some calculation, Eq. (9) becomes

$$A'(\theta_0,\varphi_0)=\frac{1}{2}\int\delta\left(\frac{\hat{\xi}(\theta_0',\varphi_0')\cdot\hat{r}(\theta,\varphi)}{[\sin^2\theta_0'(\sin^2\varphi_0'+\alpha^{-2}\cos^2\varphi_0')+\gamma^{-2}\cos^2\theta_0']^{1/2}[\sin^2\theta(\sin^2\varphi+\alpha^2\cos^2\varphi)+\gamma^2\cos^2\theta]^{1/2}}\right)\times\frac{\alpha\gamma r^2(\theta,\varphi)\sin\theta\,d\theta\,d\varphi}{[\sin^2\theta(\sin^2\varphi+\alpha^2\cos^2\varphi)+\gamma^2\cos^2\theta]^{1/2}}. \tag{10}$$

[5] F. M. Mueller and M. G. Priestley, Phys. Rev. 148, 638 (1966).

If we use the property of the δ function that $\delta[xf(x)] = [\delta(x)/f(x)]$, where $f(x)$ is a smoothly varying function that has no zeros, Eq. (10) becomes

$$A'(\theta_0,\varphi_0)=\alpha\gamma[\sin^2\theta_0'(\sin^2\varphi_0'+\alpha^{-2}\cos^2\varphi_0') +\gamma^{-2}\cos^2\theta_0']^{1/2}A(\theta_0',\varphi_0'). \quad (11)$$

We drop the subscript and operate on all angles with T^{-1}, obtaining

$$A'(T^{-1}\theta,T^{-1}\varphi)=\alpha\gamma[\sin^2\theta(\sin^2\varphi+\alpha^{-2}\cos^2\varphi) +\gamma^{-2}\cos^2\theta]^{1/2}A(\theta,\varphi). \quad (12)$$

We rewrite Eq. (7a) for comparison

$$r'^2(T\theta,T\varphi)=[\sin^2\theta(\sin^2\varphi+\alpha^2\cos^2\varphi) +\gamma^2\cos^2\theta]r^2(\theta,\varphi). \quad (7a')$$

Equations (12) and (7a') are the sought after relations between areas and radii in the transformed and untransformed system.

An alternate approach to removing the nearly ellipsoidal character of a data set makes use of the analytical character of such a surface. Assume that the area data $A(\theta,\varphi)$ are expanded as follows:

$$A(\theta,\varphi)=A_e(\theta,\varphi)+\sum_{l,m}[\beta_{l,m}{}^gC_{l,m}{}^g(\theta,\varphi) +\beta_{l,m}{}^uC_{l,m}{}^u(\theta,\varphi)], \quad (13)$$

where $A_e(\theta,\varphi)$ is the area of an ellipsoid (or any other analytic surface) which best represents the data, and the remaining terms account for deviations from this surface. On applying the inversion theorem we have

$$r^2(\theta,\varphi)=r_e^2(\theta,\varphi)+\sum_{l,m}[\gamma_{l,m}{}^gC_{l,m}{}^g(\theta,\varphi) +\gamma_{l,m}{}^uC_{l,m}{}^u(\theta,\varphi)], \quad (14)$$

where the $\gamma_{l,m}$ are determined using Eq. (4). Rather than representing $A_e(\theta,\varphi)$ and $r_e^2(\theta,\varphi)$ as expansions as in Eqs. (1) and (2) (which do not in general terminate), it is more convenient to use the following analytical expressions (appropriate for ellipsoids):

$$A_e(\theta,\varphi)=\pi[\sin^2\theta(a^{-2}c^{-2}\sin^2\varphi+b^{-2}c^{-2}\cos^2\varphi) +a^{-2}b^{-2}\cos^2\theta]^{-1/2}, \quad (15)$$

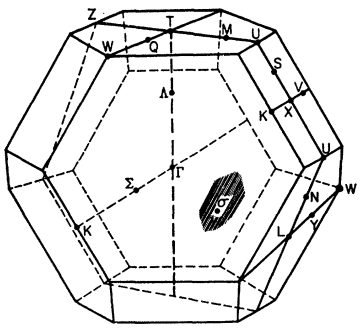

FIG. 1. Brillouin zone for the $A7$ crystal structure appropriate to Sb and As. The points, lines, and planes of symmetry are indicated.

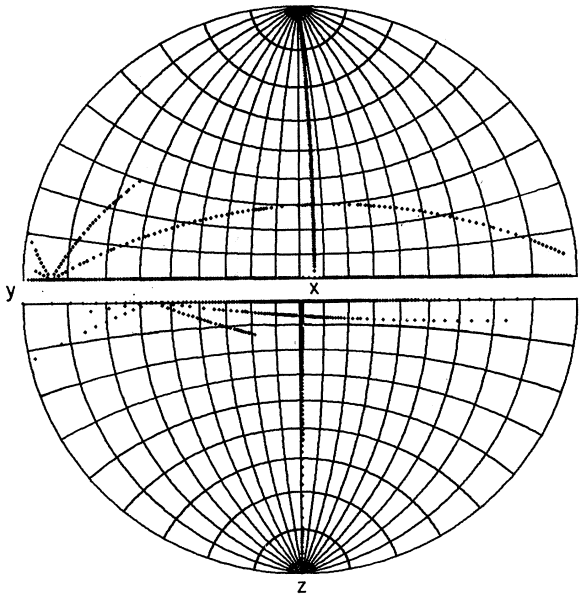

FIG. 2. Stereogram of the As $A7$ crystal structure with the x, y, and z axes corresponding to that of the least-squares fit. The upper half shows the available area data points in the system before the spherical mapping was applied, while the lower half shows these data points in the transformed system. Note the concentration of points in the transformed system near the center of the stereogram indicating how the angles are "stretched out" near the large radii sector.

$$r_e^2(\theta,\varphi)=[\sin^2\theta(b^{-2}\sin^2\varphi+a^{-2}\cos^2\varphi) +c^{-2}\cos^2\theta]^{-1}, \quad (16)$$

where a, b, and c are defined in Eq. (5). Obviously Eqs. (15) and (16) are particular cases of Eqs. (12) and (7a) when the transformed surface is a sphere. In the following we will refer to this inversion technique as the subtraction procedure.

The spherical mapping procedure and the subtraction procedure will each have particular cases suited to them. We feel the spherical mapping procedure is the best for Sb and As for reasons which will be discussed in the following section.

INVERSION OF ARSENIC AND ANTIMONY ELECTRON SURFACE

The dHvA data on antimony[6] and arsenic[7] are quite accurate and complete. The field rotation technique was used in these measurements and thus the anisotropy of the areas are known with high precision. Field sweeps with the end points determined by nuclear magnetic resonance were also included in these measurements and thus the absolute accuracy is high. The electron surface at the point L in As and Sb has the point group symmetry C_{2h} and is thus invertible. The hole surface contains only mirror symmetry and con-

[6] L. R. Windmiller, Phys. Rev. **149**, 472 (1966).
[7] M. G. Priestley, L. R. Windmiller, J. B. Ketterson, and Y. Eckstein, Phys. Rev. **154**, 671 (1967).

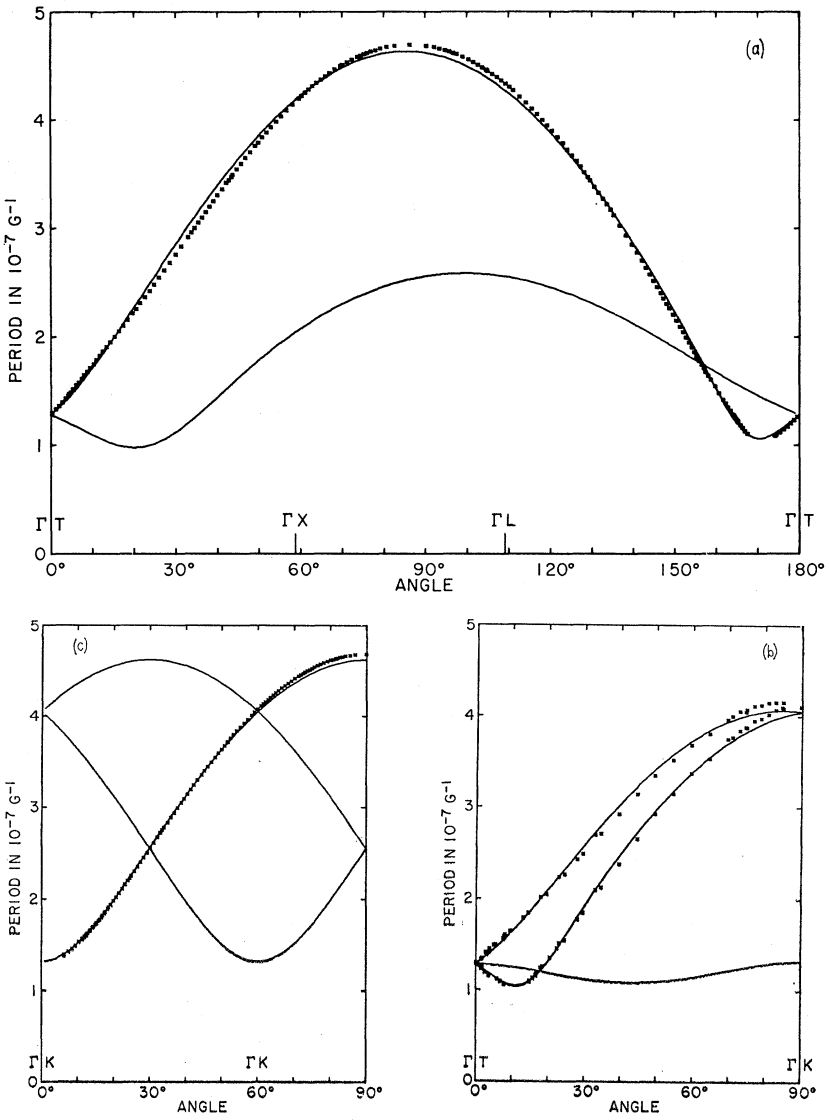

FIG. 3. Arsenic dHvA data together with the fit: (a) magnetic field in the binary plane; (b) magnetic field in the bisectrix plane; (c) magnetic field in the trigonal plane.

sequently this surface cannot be inverted to obtain radii. The anisotropy of the radii of the electron surface is quite large (on the order of 6:1) and thus the series (1) and (2), when applied directly to the data, will converge quite slowly. On the other hand, the surfaces are reasonably ellipsoidal and appear to be ideal candidates on which to apply the new spherical mapping procedure contained in Eq. (12).

We proceed as follows: First, approximate values of α, γ, and φ_0 (the angle of rotation necessary to align the ellipsoid in the x-y plane) are determined from the data. At this point we note that it is possible, for all of the groups considered, to make all of the $l=2$ terms in the expansion vanish by a proper choice of the transformation parameters α, γ, etc. Finite values for the $l=2$ components imply that all of the ellipsoidal character of the surface has not been transformed away. Thus, by adjusting the transformation parameters (the number of which coincides with the number of $l=2$ terms) we can make the $l=2$ components vanish. After the approximate values of α, γ, and φ_0 have been determined, the area data are mapped into the transformed system using Eq. (12). Next the data are least-squares fitted to a finite series of the form given in Eq. (2). The radii in the transformed system are then evaluated using Eqs. (4) and (1). The radii are then mapped back into the untransformed system using Eq. (7a). These procedures accomplish the inversion.

Arsenic and antimony have the trigonal $A7$ crystal structure. The Brillouin zone for this structure is shown in Fig. 1. The Λ line formed by the points Γ and T is the threefold or trigonal axis and the Σ line formed by Γ and K is a twofold or binary axis. A mutually perpendicular third axis is called the bisectrix axis. The σ plane formed by the points L, Γ, and T has mirro

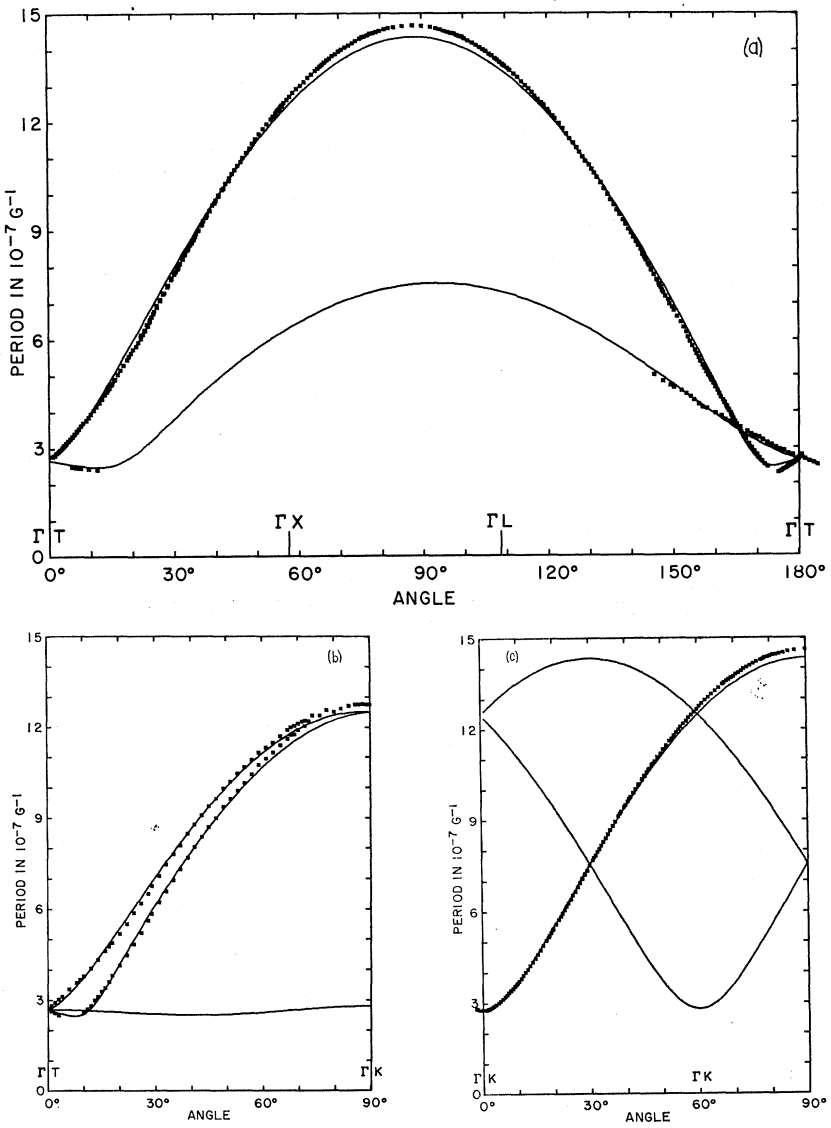

FIG. 4. Antimony dHvA data together with the fit: (a) magnetic field in the binary plane; (b) magnetic field in the bisectrix plane; (c) magnetic field in the trigonal plane.

symmetry. The electron surface is centered on the point L. The Y line formed by the points L and W is a twofold axis. Since L lies in the mirror plane, the point group symmetry of L is $2/m$ or C_{2h}. Owing to the threefold symmetry about the Λ axis there are three sets of points L, not related by inversion through Γ, and thus the electron FS consists of three ellipsoids. Similarly, there are three equivalent binary (and bisectrix) axes. The three ellipsoids transform into one another on making $\pm 120°$ rotations about the Λ line.

dHvA data in As and Sb were taken in the planes perpendicular to the trigonal, binary, and bisectrix axes. The ellipsoid having its mirror plane coinciding with the mirror plane formed by the particular choice of trigonal-bisectrix axes used to define the data will be called the principal ellipsoid. The remaining two ellipsoids will be referred to as the nonprincipal ellipsoids. For the magnetic field in the plane perpendicular to the Λ axis the extremal area of the three ellipsoids will in general be different. The same is true for the field in the plane perpendicular to the bisectrix axis.

TABLE II. Expansion coefficients.

	Arsenic	Antimony
α	0.224	0.157
γ	0.805	0.827
φ_0	−99.0	−96.0
$\gamma_{0,0}$	5.466×10^{-3}	16.933×10^{-4}
$\gamma_{2,0}$	-0.278×10^{-3}	-0.140×10^{-4}
$\gamma_{2,2^g}$	0.302×10^{-3}	-0.780×10^{-4}
$\gamma_{2,2^u}$	-0.393×10^{-3}	-2.540×10^{-4}
$\gamma_{4,0}$	-0.588×10^{-3}	-0.144×10^{-4}
$\gamma_{4,2^g}$	-0.572×10^{-3}	-0.061×10^{-4}
$\gamma_{4,2^u}$	0.011×10^{-3}	1.161×10^{-4}
$\gamma_{4,4^g}$	0.150×10^{-3}	-0.198×10^{-4}
$\gamma_{4,4^u}$	0.286×10^{-3}	1.240×10^{-4}

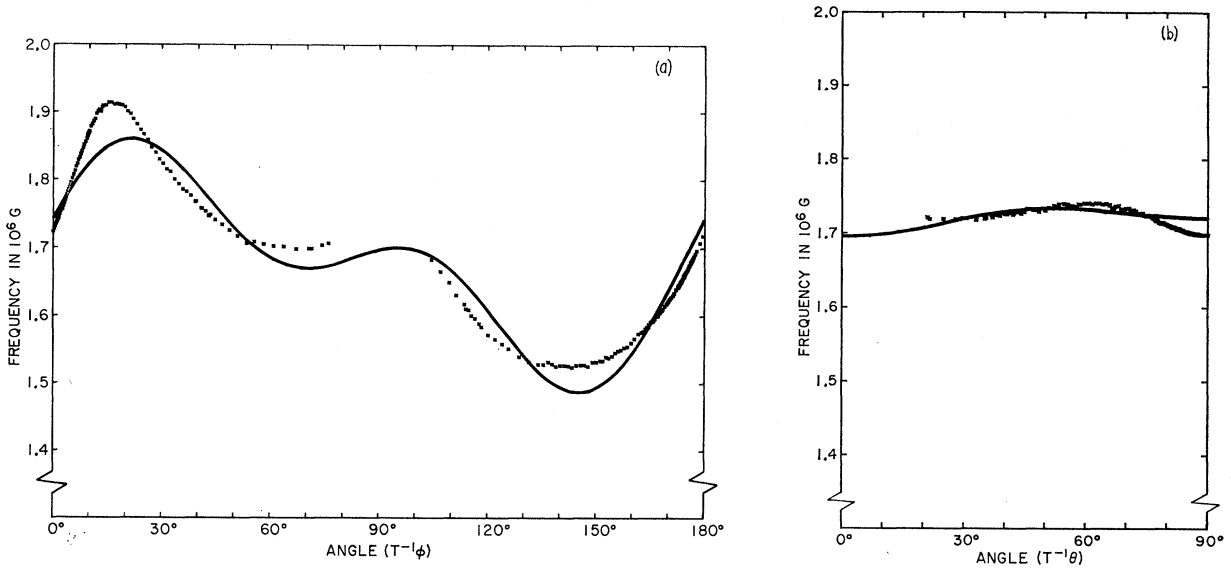

FIG. 5. Transformed dHvA data for As as a function of the angles $T^{-1}\theta$ and $T^{-1}\varphi$: (a) magnetic field in the binary plane; (b) magnetic field in the trigonal plane.

For the field in the plane perpendicular to the binary axis the extremal areas of the two nonprincipal ellipsoids are identical, due to the σ mirror plane.

In order to transform the data into the coordinate system necessary to perform the spherical mapping, three distinct coordinate rotations are performed. Initially, we choose the Λ axis as the z axis and Σ axis as the x axis. We must transform the data on the nonprincipal ellipsoids into equivalent data on the principal ellipsoid. This is accomplished by $\pm 120°$ rotations about the z axis for the nonprincipal data. Next, a 90° rotation about the bisectrix axis is performed such that the new z axis coincides with the binary axis. As mentioned earlier, the choice of the x axis is arbitrary for the C_{2h} group. We have therefore rotated the coordinate system by an angle φ_0 in clockwise direction such that the long axis of the ellipsoid coincides with the new x axis. This completes the three rotations and the principal "ellipsoid" is now oriented in its "principal-axis system" with the z axis the twofold axis.

For arsenic, data on all three ellipsoids were available in the trigonal plane. For the binary plane only the principal ellipsoid data were available. For the bisectrix plane the two nonprincipal ellipsoids were observed,

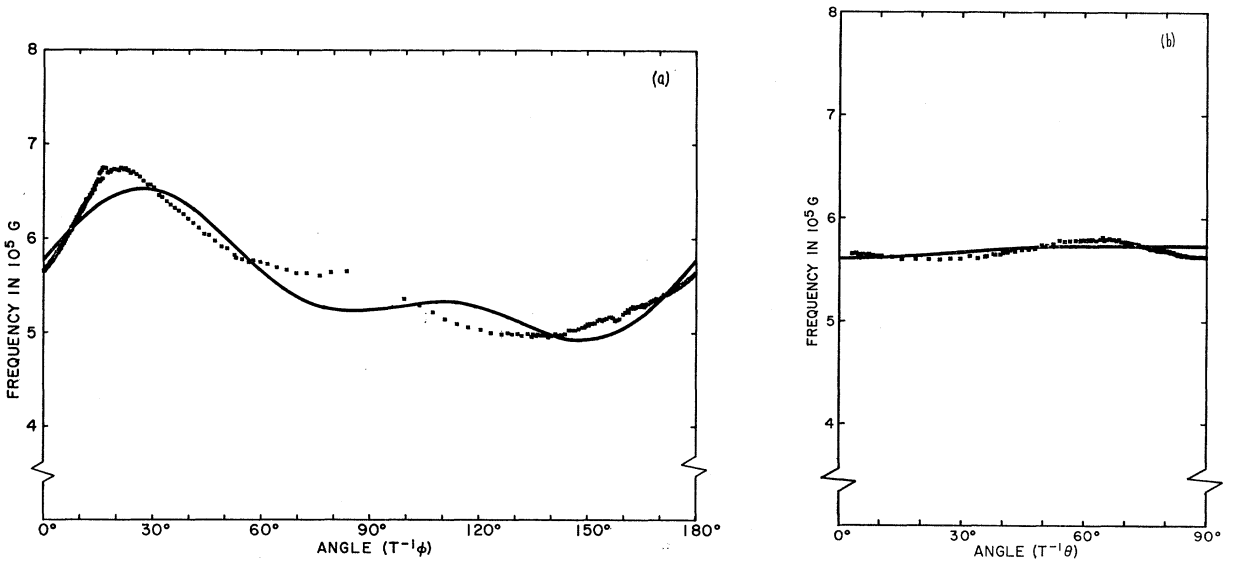

FIG. 6. Transformed dHvA data for Sb as a function of the angles $T^{-1}\theta$ and $T^{-1}\varphi$: (a) magnetic field in the binary plane; (b) magnetic field in the trigonal plane.

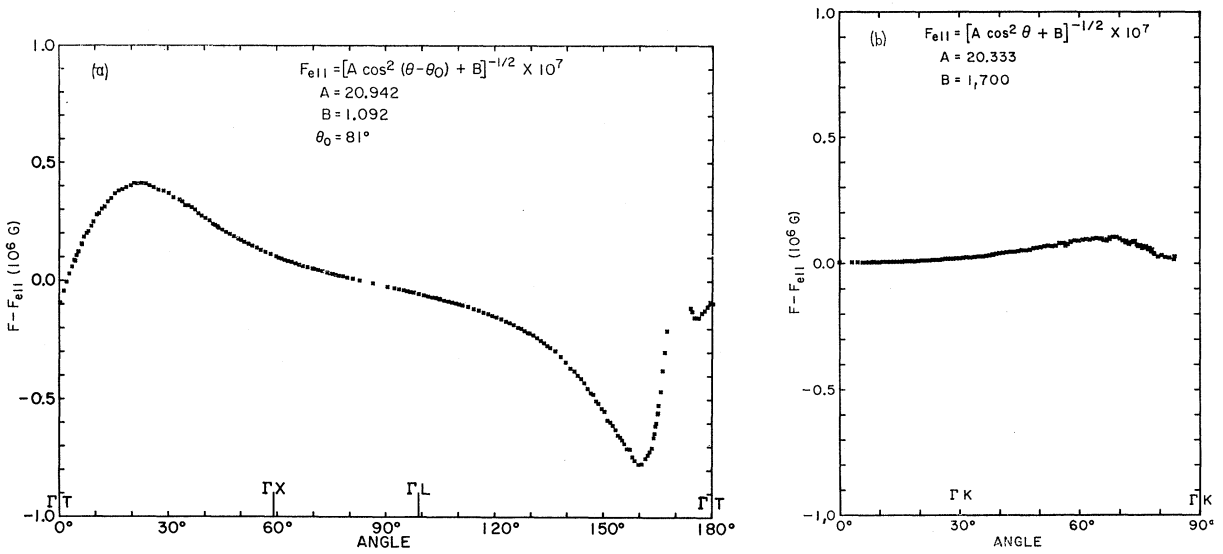

FIG. 7. Deviation of the area from an ellipsoidal fit for the principal ellipsoid in As: (a) magnetic field in the binary plane; (b) magnetic field in the trigonal plane.

but the principal ellipsoid was not. For Sb, data on all three ellipsoids were also available for the trigonal plane. For the binary plane the principal ellipsoid was observed together with a small portion of the single degenerate nonprincipal branch. For the bisectrix plane only data on the nonprincipal ellipsoid were available.

The number of expansion coefficients, which may be determined in Eqs. (1) and (2), depends on the quantity, accuracy, and angular distribution of the available data points in a nontrivial way. It was observed empirically that with the available data we could fit all the $l=0$, 2, and 4 terms (a total of nine coefficients). When an attempt was made to expand the fit to include all of the $l=6$ terms, negative values of $r^2(\theta,\varphi)$ resulted. A similar phenomenon was observed by Mueller and Priestley.[4] It was observed that the $l=6$, $m=0$ term could be reliably determined, however. No attempt was made to investigate which of the higher coefficients could be determined, since this would yield an incomplete set—a procedure which in our opinion is unjustified. The problem stems from having an insufficient data set. Ideally, one would like to have data points which are distributed densely over the unit sphere. Furthermore, since the data are fitted in

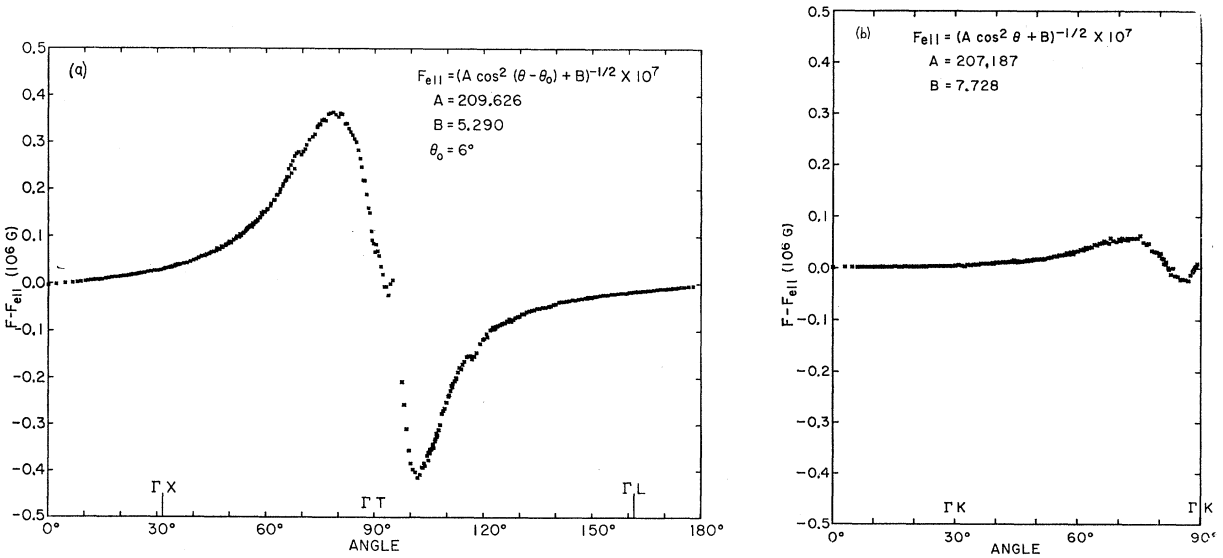

FIG. 8. Deviation of the area from an ellipsoidal fit for the principal ellipsoid in Sb: (a) magnetic field in the binary plane; (b) magnetic field in the trigonal plane.

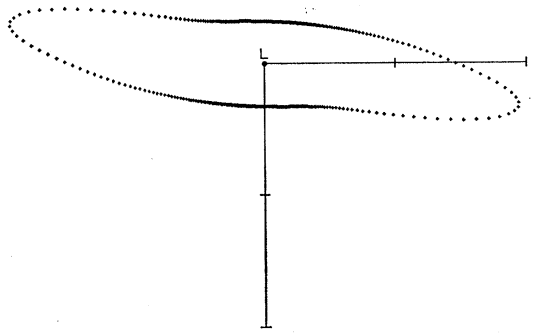

FIG. 9. Cross section in the mirror plane of the electron surface of As. The scale is in 0.1 a.u.

the transformed systems, the distribution of data points should be favorable to this system. Figure 2, a stereographic projection where the x, y, and z axes correspond to those used in our least-squares fit, shows in the upper half the data points at which area measurements were available. The lower half shows the corresponding data points in the transformed system. Observe that while some of the data points appear to cover adequately the inner portions of the basic wedge in the untransformed system, the same is not true of the transformed system, i.e., the planes in which data were taken are not well chosen from the standpoint of the transformed system. The same amount of data would presumably have allowed a higher-order fit had the data planes been chosen more favorably. We hasten to point out, however, that this does not necessarily mean that it would be more favorable to fit in the untransformed system using the subtraction procedure. As will shortly become apparent, the "sharpness" of the distortions is much more severe in the untransformed system and thus the fit would be more slowly convergent in this system. We must simply conclude that data over important regions of the surface are absent. Nonetheless we feel that the expansion through $l=4$ in the transformed system gives a reasonably good representation of the surface.

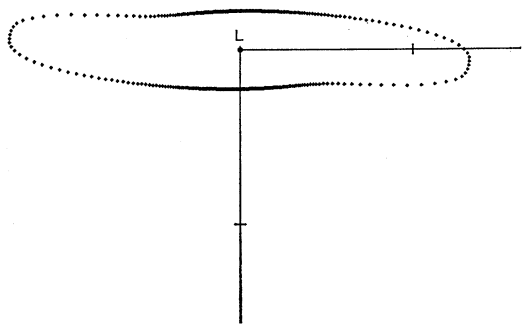

FIG. 10. Cross section in the mirror plane of the electron surface of Sb. The scale is in 0.1 a.u.

Figures 3(a), 3(b), and 3(c) show the dHvA data in As together with the fit for the magnetic field in the binary, bisectrix and trigonal planes. Figures 4(a), 4(b), and 4(c) show the dHvA data and the fit for Sb. The values of the coefficients $\gamma_{l,m}$, together with the values of α, γ, and φ_0 used, are listed in Table II for As and Sb. Figures 5(a) and 5(b) show the dHvA data for As transformed according to Eq. (12), together with the fit as a function of the angles $T^{-1}\theta$ and $T^{-1}\varphi$ for the magnetic field in the binary and trigonal planes, respectively. Figures 6(a) and 6(b) show the same thing for Sb. Observe that the deviations are reasonably well accounted for by the fit. The deviation from the ellipsoidal area is what must be fitted when using the subtraction procedure. This deviation for As is shown in Figs. 7(a) and 7(b) for the field in the binary and trigonal planes, respectively. Figures 8(a) and 8(b) show the same data for Sb. Observe that the distortion is such that a much higher-order fit would be required for an adequate representation using the subtraction procedure. In Sb and As the spherical mapping approach has the advantage that it "stretches out" the angles near regions where $r(\theta,\varphi)$ is large. Thus the deviations can be more easily accommodated by lower-order terms in the expansions and the expansion made to yield a faithful representation with a smaller number of terms.

Figure 9 shows the radius of the electron surface in the mirror plane for As. The directions parallel to the trigonal and bisectrix axis are indicated. Figure 10 shows the same slice for the Sb surface. Observe that the distortion from an ellipsoidal cross section is quite apparent. As an over-all check on the program and the transformations, the radii of a few slices (in the untransformed system) were integrated, using Simpson's rule, to calculate the area of the slice; agreement was observed to about five decimal places.

In conclusion we point out that the techniques discussed here may be easily expanded to allow the Fermi velocity to be determined from effective mass and area data.

ACKNOWLEDGMENT

We would like to thank F. M. Mueller for useful discussions and also for the use of some of his programs.